SET domain-containing protein 4: biological functions and role in genomic methylation profiles of bone marrow mesenchymal stem cells

Xiao-min Liao
Guangdong Medical University
Cai-xia Wu
Guangdong Medical University
Zhong-ming Shao
Guangdong Medical University
Shu-ya Zhang
Hainan Medical University
Yuan Zou
Guangdong Medical University
Jian-ling Yuan
Guangdong Medical University
Mu-yin Feng
Guangdong Medical University
Yan-ping Ha
Guangdong Medical University
Ru-jia Li
Guangdong Medical University
Jing-ci Xing
Guangdong Medical University
A-xiu Zheng
Guangdong Medical University
Zhi-hua Shen
Guangdong Medical University
Jun-li Guo
Hainan Medical University
Shao-Jiang Zheng
Hainan Medical University
Wei Jie (wei.jie@gdmu.edu.cn)
Gungdong Medical University https://orcid.org/0000-0002-1869-1458

Research

Keywords: SETD4, Bone marrow mesenchymal stem cells, Cell biology, Genomic methylation, Reduced representation bisulfite sequencing, Bioinformatic

Posted Date: March 5th, 2020

DOI: https://doi.org/10.21203/rs.3.rs-16128/v1

Abstract

Background: Epigenetic modification is a crucial mechanism affecting the biological function of stem cells. SETD4 is a histone methyltransferase, and its biological role in bone marrow mesenchymal stem cells (BMSCs) is currently unknown. This work was aimed to reveal the SETD4 biological role as well as its impacts on the genomic methylation profiles in BMSCs.

Methods: BMSCs were isolated form *SETD4* knockout (KO) and wild type (WT) mice that established by CRISPR/Cas9 technology. The cell proliferation, migration, myogenic differentiation and angiogenesis were tested according to appropriate biology techniques. And the Reduced Representation Bisulfite Sequencing (RRBS) method was adopted to analyze the global genomic methylation profiles of BMSCs, following bioinformatics analysis of GO functions and KEGG signaling of differential methylated CpG sites and differential methylation regions (DMRs). Finally, validation experiments were conducted to examine the expression of histone lysine methyltransferase and some representative genes.

Results: *SETD4* KO significantly promoted BMSCs proliferation, which was characterized by enhanced cell viability and increased expression of PCNA, Cyclin A2, Cyclin E1, CDK2, CDK6, Bcl2 and decreased the expression of P16, P21 and Caspase3. SETD4 deficiency impaired BMSCs migration and myogenic differentiation potentials, and even the angiogenesis via paracrine of VEGF. Compared with WT control, the overall genomic methylation of BMSCs in the *SETD4* KO group only was decreased by 0.47%. However, the changed genomic methylation covers a total of 96,331 differential methylated CpG sites and 8692 DMR, with part of them settled in promoter regions. GO and KEGG analysis revealed that differential CpG islands and DMRs in promotes impacted 270 GO functions and 34 KEGG signaling pathways, with some closely related to stem cell biology. *SETD4* KO inhibited sets of monomethylases and dimethylases for histone lysine, along with significant changes in some factors including *Nkx2.5*, *Gata4*, *Gli2*, *Grem2*, *E2f7*, *Map7*, *Nr2f2* and *Shox2* that associated with stem cell biology.

Conclusions: These results are the first to reveal that even though SETD4 changes the genome's overall methylation to a limited extent in BMSCs, it still affects the numerous cellular functions and signaling pathways, implying SETD4-altered genomic methylation serves a crucial molecular role in BMSCs' biological functions.

Background

Epigenetics is closely related to various physiological processes, such as gene transcription regulation, cell growth, stem cell differentiation, and individual development. Epigenetics also functions in many pathological conditions and systemic diseases. Histone methylation is considered to be one of the most critical modification mechanisms in epigenetics[1] and mainly occurs in the promoter region of the genes impacting the chromosome structure through methylation modification, thereby regulating gene expression. Methyltransferase is a crucial enzyme for histone modification, and histone arginine methyltransferases (HRMTs) and histone lysine methyltransferases (HKMTs) are the main types [2, 3].

SET domain-containing protein 4 (STED4) is a number of SET gene families that process histone and non-histone methyltransferase activity. Previous reports have revealed that SETD4 over-expression controls cancer cell proliferation [4, 5] and the cell quiescence via H4K20me3 catalysis [6, 7]. Very recently, SETD4-catalyzed H3K4me1 and H3K4me2 were also documented to be closely associated with the release of inflammatory cytokines in macrophage [8]. These limited reports have highlighted the vital role of SETD4 in cell biology, but to date, its biological effects, clinical targeting significance and mechanisms are mostly unclear.

Bone marrow mesenchymal stem cells (BMSC) are an auspicious kind of seed cell in tissue engineering involved in a wide range of functions. A vast number of clinical trials have shown that transplantation of BMSCs for tissue damage repairing is safe and effective. Due to the shortcoming in de novo cell differentiation in vivo, the mechanisms regarding BMSCs infusion in tissue injury repair appear to be mostly related to its paracrine effects [9]. The ideal effect of stem cell transplantation for tissue damage depends on the cell transplantation rate, differentiation, and paracrine protective factors. Epigenetics in mesenchymal stem cell differentiation has attracted considerable attention, and most investigations have been focused on osteogenic, adipogenic and cardiogenic differentiation [10–12], highlighting epigenetic modification in stem cell biology and regenerative medicine[13].

In this investigation, we identified the role of SETD4 in the biological function of BMSCs, and we further uncovered the epigenetic modification about SETD4-impacted genomic methylation profiles in BMSCs. Our results provide insight into revealing the value of the targeted intervention of methyltransferase SETD4 in BMSC-based regenerative medicine.

Methods

Established *SETD4* knockout mouse on the Cyagen platform

Customized *SETD4* gene (NCBI ID, 224440) conventional knockout C57BL/6 mice were provided by the Cyagen Biosciences Inc. (Suzhou, China). We used CRISPR/Cas9 technology to edit mouse *SETD4* gene. And exons 6–8 of SETD4 gene were selected as targets. Designed sgRNAs and *Cas9* mRNA vectors were electrotransfected into the fertilized egg; embryo was transferred after *in vitro* fertilization to obtain *SETD4* knockout mice. Genotyping was performed as conditional PCR methods using mouse tail genomic DNA and further identified by DNA sequencing. The primers for genotyping were as follows: forward (F): GTTGGAGAGGAGTAAAGAGCCG; reverser 1(R1): TGAAGAGTCCCACAGGCTCAAC; reverser 2(R2): TGCAGAGGAGATCCCAGTATC. SPF-level heterozygous mice were bred at the Experimental Animal Center of Guangdong Medical University, and the qualified mice were divided into homozygous ($SETD4^{-/-}$, KO), heterozygous ($SETD4^{+/-}$) and wild type ($SETD4^{+/+}$, WT) groups. The diagram of the *SETD4* gene knockout is shown in Fig. 1a.

Isolation, culture and identification of BMSCs from WT and *SETD4* KO mice

BMSCs were isolated, cultured and identified as per published protocols [14, 15]. Briefly, after anesthesia with Avertin, the mice (male, weighting » 20 g) were sacrificed by cervical dislocation. Isolated femur and tibia were grinded and crushed, and the cells were suspended with cold DMEM medium (HyClone) and filtered with 70-μm filters, then cell masses were treated with red blood lysing buffer (#R7757, Sigma) for 5 min at room temperature. After washing with cold DMEM medium twice, cells were suspended with mouse BMSC-specific medium (#MUBMX-90011, Cyagen Biosciences Inc.) and plated in an incubator at 37°C with saturated humidity. For normoxic culture, cells were conventionally maintained (21% O_2, 5% CO_2); for hypoxic culture, cells were maintained in a hypoxic incubator (Galaxy 48R, Eppendorf, Germany) at 2% O_2, 5% CO_2 and 93% N_2. Cells in the third passage (P3) were subjected to flow cytometrical analysis of its immunophenotype (CD34, CD45R, CD73 and CD90), and cells in P5-P6 were subjected to associated experiments.

Induced differentiation of BMSCs

We used Transforming growth factor b1 (TGF-b1) plus 5-Aza-2'-deoxycytidine (5-Aza) to induce myogenic differentiation[12]. For myogenic differentiation, 1×10^5 cells were seeded on 6-well plates, and then cells were treated with combination of TGF-b1 (5 ng/mL, #100-21, PeproTech, USA) plus 5-Aza (5 μmol/L, #11390, Sigma-Aldrich, Germany) for 24 h under normoxic condition (21% O_2), then medium was changed for DMEM supplemented with 10% FBS (Gibco), TGF-b1 for continuous 14 days. The cells were subjected to RNA isolation and quantitative RT-PCR analysis of the expression of differentiation-related markers of cardiomyocyte lineage as following: *Nkx2.5*, *Gata4*, *Mef2a*, *ANP*, *CX43* and *cTnT*.

Cell viability assessment by CCK-8 assay

CCK-8 assay was used to test the cell viability as previously described [16]. Briefly, BMSCs (2×10^3 cells/well in 200 μL medium) were seeded onto 96-well plates. Cells were allowed to recover overnight; the medium was changed every 3 days. At 0, 1, 2, 3 and 7 d setpoints, 10 μL of CCK-8 reagents (#SPDA-D010, Beyotime Institute of Biotechnology, Nanjing, China) was added, cells were maintained for additional 2 h, then OD values at 450 nm were measured using a microplate reader (Thermo Scientific, USA). Each group was duplicated in six wells.

Cell migration assay

Transwell migration assay was performed using 8-μm pore size polycarbonate membrane chambers (Corning, Tewksbury, MA, USA) as previously described [17]. Briefly, 2×10^4 BMSCs in total 200 μL were seeded in the upper chamber; the lower chamber contained 500 μL DMEM medium supplemented with 10% FBS. Cells were maintained for 24 h at 37°C in the incubator, and then the chambers were fixed for 15 min with 4% paraformaldehyde and stained with 0.1% crystal violet, followed by washing with PBS twice. Cells on the upper surface of the membrane were removed. The images were photographed with a microscope (Leica, Wetzlar, Germany) at 20× objective field, and the number of migrated cells on the

lower surfaces of the membranes was counted. Each experimental group was repeated in three chambers, and cell numbers from a total of nine representative fields were obtained.

Assessment of angiogenic factors by ELISA

A total of 2×10^5 BMSCs were seeded on 6-cm dishes, and cells were maintained under normoxia (21% O_2) and hypoxia condition (2% O_2) for 1, 3 and 7 d. Cell culture supernatant was collected and subjected to ELISA analysis of VEGF levels, according to the manufacturer's instructions. Mouse VEGF ELISA kit (#RRV00, R&D, USA) was used.

Tube formation assay

HUVECs (presented by Dr. Xujuan Zhang, Department of Physiology, Guangdong Medical University) were maintained with DMEM medium supplemented with 10% FBS. Cells in the logarithmic growth phase were used for experiments. A total of 300 μL Matrigel (#9056007, Corning, USA) was added in a 24-well plate and coated at 37°C for 30 min. A total of 5×10^4 well HUVECs were seeded per wells. After 10 min of cell attachment, the media was replaced by the WT and *SETD4*-KO BMSC conditional media. Images were acquired after 6 h of cell culture under a 10× microscope objective. The tube formation images were analyzed by the software Image J (https://imagej.nih.gov/ij/).

RNA isolation, reverse transcription (RT) and PCR

Cellular total RNAs were extracted using TRIZOL reagent (#15596-026, Ambion, USA) and quantitated by SimpliNano (Biochrom, Germany). Total 200 ng RNA was used to generate cDNA using an RT kit (#K1622, Fermentas, USA). Quantitative PCR was performed using a LightCycler 480 II machine (Roche, Swish). In addition, the 20 μL reactive mixture included 10 μL SYBR Green I PCR Master Mix (#QPK-201, TOYOBO, Japan), 0.4 μL forward primer (10 μM), 0.4 μL reverse primer (10 μM), 2 μL cDNA and 7.2 μL ddH_2O. PCR amplification was performed as follows: 95°C for 1 min and then 45 cycles of 95°C for 5 s and 60°C for 20 s. 2^{-DDCT} method was used to determine the levels of mRNAs. Primers (5'–3') spanning exon-exon junction are listed as follows:

SETD4, CATGTGCAGGTAAAAGCGGC, CTCCTGGTGCTTCCTACAGC;

VEGF-A, CAAACCTCACCAAAGCCAGC, CACAGTGAACGCTCCAGGAT;

Gata4, AGCTCCATGTCCCAGACATTC, GCTGTTCCAAGAGTCCTGCT;

Nkx2.5, CACCACTCTCTGCTACCCAC, AGCGCGCACAGCTCTTTT;

Mef2a, GCAGTGCAAGTGGGATGTTG, CCCTTGCTTGATGGGGGAAT;

cTnT, TTCAGAGGGAGAGCCGAGAG, GCACCAAGTTGGGCATGAAG;

CX43, TGAAAGAGAGGTGCCCAGAC, ACACGTGAGCCAAGTACAGG;

ANP, ATCCTGTGTACAGTGCGGTG, TTCGGTACCGGAAGCTGTT;

SM22α, GGTCCATCCTACGGCATGAG, TGCTCCTGGGCTTTCTTCAT;

α-SMA, CCTTCGTGACTACTGCCGAG, AATGCCTGGGTACATGGTGG;

Gli2, AGCCTTCACCCACCTTCTTG, TCTGCTTGTTCTGGTTGGCA;

Grem2, CATTGCAGGATGTTCTGGAAGC, CTGGTGATGCCACCTCTCTG;

Map7, CAGTGGAGATCCAGACAGGC, TAACAACGCTGCTCTCCCAG;

E2f7, TGAACTCCCTGCAGCTTGAC, AGCTCGGATAGCGAGCTAGA;

Shox2, GAGGCCCGAGTACAGGTTTG, CGCCTGAACCTGAAAGGACA;

Foxo6, CTGGAAGAACTCCATTCGGCA, AGGTGCAGCTGCTTCTTCTT;

Klf14, GAGGATGAGCTCTCTGACGC, GGTACGCTGGTGTGACTTGA;

Nr2f2, GCATGAGACGGGAAGCTGTA, ACAGGTACGAGTGGCAGTTG;

Dyrk3, GGCTAAATATTACCACTGAGCCAC, CTCCAGCTTCTCGTAGGCAG;

b-actin, GTTGGAGAGGAGTAAAGAGCCG, TGAAGTGTCCCACAGGCTCAAC.

Western blot

Cells were lysed with RIPA buffer (Beyotime Institute of Biotechnology). A sample of 35 μg total proteins were subjected to 12% SDS-PAGE and then transferred to PVDF membranes (Millipore, USA). After washing with TBST twice, the membranes were incubated with 5% skim milk powder in TBST at 37°C for 1 h and then primary antibodies at 4°C overnight. The primary antibodies include SETD4 (1:500, #173906, Abcam, UK), PCNA (1:500, #2586, CST, USA), Caspase3 (1:1000, #9662, CST), Bcl2 (1:500, #12789-1-AP, Proteintech, Wuhan, China), CyclinA2 (1:1000, #18202-1-AP, ProteinTech), CyclinB1 (1:500, #55004-1-AP, ProteinTech), CyclinD1 (1:2000, #60186-1-Ig, ProteinTech), CyclinE (1:500, #11554-1-AP, ProteinTech), CDK2 (1:500, #10122-1-AP, ProteinTech), CDK4 (1:500, #11026-1-AP, ProteinTech), CDK6 (1:500, #14052-1-AP, ProteinTech), P16 (1:500, #10883-1-AP, ProteinTech), P21 (1:500, #10355-1-AP, ProteinTech), H4K20me1 (1:5000, #ab177188, Abcam), H4K20me2 (1:2000, #ab78517, Abcam), H4K20me3 (1:1000, #ab177190, Abcam), H3K4me1 (1:1000, #BS1174, Bioword, Nanjing, China), H3K4me2 (1:2000, #ab32356, Abcam), H3K4me3 (1:1000, #ab213224, Abcam), H3K27me1 (1:1000, #BS7235, Bioword), H3K27me2 (1:1000, #BS7236, Bioword), H3K27me3 (1:1000, #ab192985, Abcam), H3K36me1 (1:10,000, #ab176920, Abcam), H3K36me2 (1:5000, #ab176921, Abcam), H3K36me3 (1:1000, #BS7239, Bioword), H3K79me1 (1:10,000, #ab177183, Abcam), H3K79me2 (1:2500, #ab177184, Abcam), H3K79me3 (1:1000, #ab208189, Abcam), b-actin (1:1000, 60008-1-Ig, ProteinTech) and GAPDH (1:1000, #SC-32233, Santa Cruz, USA). After washing with TBST twice, the membranes were incubated

with HRP-conjugated IgGs (1:5000, #SA00001-10, #SA00001-2, ProteinTech) for 1 h at 37°C. Bands were visualized using ECL reagents (Thermo Fisher, USA) and analyzed with a gel analysis system (Tanon; Shanghai, China).

DNA methylation analysis by Reduced Representation Bisulfite Sequencing (RRBS) on Genechem platform

BMSCs were cultured on 6-cm dishes at 37°C for 72 h, marked as WT and *SETD4* KO groups (n = 3). Cells were harvested and immediately frozen in liquid nitrogen for 30 min and sent to Genechem Co, Ltd. (Shanghai, China), to assess the genomic DNA methylation status. The experimental protocol steps were as follows: (1) 500 ng genome DNA in each group was digested overnight at 37°C using restriction enzyme Msp1 (Sigma Aldrich) in order to enrich the CpG islands and other CpG methylation-intensive areas. (2) The digested product was purified using an Axygen PCR Cleaner Kit; (3) Repair was ended, and A was added to 3'-terminal of product; (4) Product was re-purified using the Axygen PCR Cleaner Kit (Corning); (5) Methylation linker was added; (6) Agarose electrophoresis and DNA fragments with sizes ranging from 160 to 400 bp were extracted using a GeneJE T Gel Extraction Kit (ThermoFisher Scientific); (7) Bisulfite treatment was conducted using an EZ DNA Methylation-Gold kit (Zymo Research, USA); (8) Bisulfite-converted library with conversion rate > 98% was subjected to PCR amplification, magnetic bead purification and Qubit measurement;(9) Single-read sequencing was conducted using an Illumina Hiseq. The raw data obtained by Illumina Hiseq sequencing were converted into sequence data by Base Calling, and the results were stored in FASTQ file format. Clean reads were compared with reference mouse genome Mus_musculus. GRC38. After the quality check, the R package methylKit was used to analyze the differential methylation status and functional annotation, which include coverage of different CpG, distribution of differential methylated CpG, distribution of CpG in different characteristic regions, difference in CpG methylation between different samples and differential methylation regions (DMRs). David Online Software was adapted to document genes' function (GO enrichment and annotation) and signal pathways (KEGG signaling enrichment and annotation).

Statistical analysis

Statistical analyses were conducted using GraphPad Prism (Version 7.0, GraphPad Software, CA, USA). Data are expressed as means ± SEM. Differences between two groups were analyzed using umpired Student's t tests. For comparisons between multiple groups, ANOVAs were used followed by Tukey's multiple comparisons test. $P<0.05$ was considered to be statistically significant.

Results

Morphology and immunophenotype of BMSCs from WT and SETD4 KO mouse

Mouse *SETD4* gene was selected as the editing target, and exons 6–8 were designed to be deleted using CRISPR/Cas9 technology (Fig. 1a). After the pups were grown up, mouse tail DNA was used for genotypic identification, and the identification strategy is shown in Fig. 1b and 1c. We found that the positive

animals of *SETD4* KO displayed a deletion of 4044 bp DNA fragment (Fig. 1d), supporting the success in establishing *SETD4* KO mice. Then the BMSCs were isolated from wild type (WT), heterozygote and *SETD4* KO mice, and western blot results confirmed changes in the expression of the SETD4 protein in corresponding BMSCs (Fig. 1e). Microscopically, the morphology of BMSCs in WT and KO groups was not significantly different (Fig. 1f). Immunostaining of BMSC markers indicated both WT and *SETD4* KO cells were positive for CD90, CD73 and CD45R, and negative for CD34 (Fig. 1g).

Deficiency in *SETD4* promotes BMSCs proliferation but not migration

CCK-8 assay was used to determine the viability of BMSCs. As shown in Fig. 2a, the viability of the KO group was significantly higher than that of the WT group since 3 d post-cell seeding, suggesting *SETD4* deficiency was beneficial for BMSCs proliferation. Because cell proliferation was tightly associated with changes in cell cycle and apoptosis-associated proteins, we then detect the levels of cell cycle and apoptosis-associated proteins. As shown in Fig. 2b and 2c, *SETD4* KO up-regulated PCNA, the marker for cell proliferation, and increased a panel of cell cycle-associated proteins, like CDK6, CyclinA2 and CycinD1. In contrast, P16 and P21 were decreased. Interestingly, we detected an increase of Bcl2 and a decrease of total Caspase3 in *SETD4* KO cells, even under normal cell culture conditions, but we failed to detect the active Caspase3. We further examined the migratory ability of BMSCs. As shown in Fig. 2d, the transwell migration assay revealed that BMSCs in the *SETD4* KO group displayed much-weakened ability in migration than that of the WT group.

SETD4 is a requirement for BMSC-promoted angiogenesis

Considering that one crucial role of BMSCs in tissue injury repair is the promotion of angiogenesis, we assessed the contribution of *SETD4* in BMSC's ability to secrete VEGF, a key pro-angiogenic factor. We found that WT BMSCs can secrete VEGF to the supernatant of culture medium to some extent with the prolongation of culture time, and this potential is more pronounced when cultured under hypoxic conditions. Compared with WT cells, *SETD4* KO BMSCs displayed a significant inhibited VEGF secretion under both normoxia and hypoxia (Fig. 2e). *VEGF-A* mRNAs in BMSCs further confirmed this tendency (Fig. 2f). Using the angiogenic growth factor-enriched supernatant, we further tested the HUEVC tube formation ability, which showed supernatant from WT BMSCs stimulated, while supernatant from *SETD4* KO BMSCs weakened, HUEVC tube formation potentials (Fig. 2g).

SETD4 KO inhibited myogenic differentiation of BMSCs

Under the stimulus combining 5-Aza and TGF-b1 for 14 d, WT BMSCs can differentiate *in vitro* into cardiomyocyte-like and smooth muscle cells (SMC, Fig. 3), as evidenced by the enhanced expression of cardiomyocyte lineage markers *(Nkx2.5*, *Gata4*, *ANP*, *CX43*) and SMC lineage marker (*a-SMA*, *SM22a*). Although the stimulation combining 5-Aza and TGF-b1can also induce differentiation of *SETD4* KO BMSCs in a similar fashion to WT, its differentiation ability was significantly reduced. We also noticed that at the beginning of differentiation (day 1), *SETD4* KO BMSCs displayed much lower baseline levels of

differentiation than that of WT cells. Together these results suggested that *SETD4* KO inhibited BMSCs' myogenic differentiation potentials.

SETD4 KO altered BMSC genomic methylation status

Considering SETD4's role as a methyltransferase, to change the genomic methylation conditions, we, therefore, adapted RRBS to assess the degree of genomic methylation. Through rigorous quality control (Fig. S1, Additional file 1), our RRBS results were qualified and suitable for subsequent analysis. The basic information including the original sequencing reads, the length of the reads, the number of all bases, and the clean reads after processing and the comparison information are shown in Table S1 (Additional file 2). Compared to WT cells, the average methylation of all CpG in *SETD4* KO BMSCs was decreased by 0.47%, suggesting that the single knockout of *SETD4* has limited effects on the overall genomic methylation. Further information indicated the coverage of CG of the two groups of samples was identical, and the minimum coverage was 10×, mainly concentrated between 10× and 100×, indicating that the data have high credibility (Fig. S2a, Additional file 3). It can be seen that the CG methylation of the two groups of samples is distributed at both ends, that is, mainly distributed in permethylation (90%–100%) and total unmethylation (0%–10%) (Fig. S2b, Additional file 3). Annotation of different feature areas of CpG showed that the distribution of CpG on the genome is similar in WT and *SETD4* KO cells (Fig. 4a, b). We further screened the differential site methylation CpG and annotated the gene and promoter regions. There were total 96,331 differential site methylation CpGs (Fig. 4c) and 8692 DMRs (Fig. 4d). Compared with WT, *SETD4* KO cells displayed more difference < -25% CpG sites. The complete lists for CpG sites with the difference in *SETD4* KO and WT cells are shown in Table S2 (Additional file 4). Regarding the DMRs, the complete lists for DMR between *SETD4* KO and WT cells are shown in Table S3 (Additional file 5).

Bioinformatics analysis using GO and KEGG database

Taking the difference >25% and P<0.01 or <-25% and P<0.01 as a standard, we found 2247 DMRs in the gene's promoter region (Fig. 4d). Gene function annotations and signaling pathway annotations were performed using David's online software. As shown in Fig. 5a, numbers of enriched significant GO terms in the biological process were 181, cellular components were 35 and molecular functions were 44, and the complete lists of enriched GO terms are shown in Table S4 (Additional file 6). We listed the top 15 GO terms for each classification as shown in Fig. 5b. GO:0007275 (multicellular organism development), GO:0006355(regulation of transcription, DNA-templated) and GO:0006351 (transcription, DNA-templated) were the top three GO terms in biological process classification. GO:0016020 (membrane), GO:0030054(cell junction) and GO:0005667 (transcription factor complex) were enriched in cellular component classification. Taking GO:0005667 as example, total 42 factors including *IRX4*, *HNF1B*, *HOXA11*, *SOX2*, *HOXD12*, *HOXB13*, *PAX3*, *SOX9*, *MEIS1*, *MSX2*, *TAL1*, *BARX2*, *GATA5*, *HAND2*, *GATA4*, *POU4F3*, *NKX2-1*, *POU3F2*, *NOBOX*, *SOX17*, *POU3F1*, *SCX*, *NKX2-5*, *PITX1*, *ALX1*, *FOXD3*, *PITX2*, *CEBPA*, *DMBX1*, *RARG*, *LBX1*, *EPAS1*, *TBX3*, *RCOR2*, *MAFB*, *PTF1A*, *SMAD5*, *SMAD3*, *MSX1*, *SALL4*, *SKOR2* and *ZFHX3* were enriched. A total of 44 enriched GO terms including GO: 0043565 (sequence-specific DNA

binding) and GO: 0005515 (protein binding) in molecular function classification suggested *SETD4* plays a crucial role in molecular function.

We enriched 62 KEGG signaling, 34 of which were statistically different (Fig. 5c). The total KEGG signaling is listed in Table S5 (Additional file 7). Among the 34 KEGG signaling, mmu04024(cAMP signaling pathway), mmu04015(Rap1 signaling pathway), mmu04810(Regulation of actin cytoskeleton), mmu04550(Signaling pathways regulating pluripotency of stem cells), mmu04510(Focal adhesion), mmu04390 (Hippo signaling pathway) and mmu04010 (MAPK signaling pathway) have been reported to be closely related to stem cell biology.

Validation of representative genes and HKMTs

Our investigation focused on the enriched GO term (0005667, transcription factor complex), and two factors named *Nkx2.5* and *Gata4* were also included (Table S4, Additional file 6). These two transcriptional factors also function in cardiomyocyte differentiation. These two factor processes multiply differentially methylated CpG sites (Table S6, Additional file 8). The baseline level of *Nkx2.5* and *Gata4* in *SETD4* KO cells was lower than that of WT cells (Fig. 3). We further assessed another nine genes with multiple different methylated CpG sites, *Gli2*, *Grem2*, *E2f7*, *Map7*, *Nr2f2*, *Shox2*, *Foxo6*, *Klf14* and *Dyrk3* (Fig. 6a; for full differential methylated CpG sites, see Table S6, Additional file 8). We found that the transcription levels of *Gli2*, *Map7*, *Shox2* and *Klf14* were increased in *SETD4* KO BMSCs, while the transcription levels of *Grem2*, *E2f7*, *Nr2f2*, *Foxo6* and *Dyrk3* were decreased in *SETD4* KO cells when compared with the WT cells (Fig. 6b). Taken *Klf14* was a sample, it just has 65 hypomethylated sites but no hypermethylated sites in its promoter region (Fig. 6a), and the level of *Klf14* mRNA therefore was significantly up-regulated in *SETD4* KO cells, this expression trend was consistent with the discipline of hypomethylation promoting gene expression. We also tested the changes in sets of HKMTs and found that *SETD4* KO BMSCs indeed processed lower levels of H4K20me1, H4K20me2, H3K4me1, H3K4me2, H3K27me2, H3K36me1, H3K36me2, H3K79me1 and H3K79me2 than WT cells, whereas the histone arginine trimethyltransferase was not significantly changed (Fig. 6c). Thus, change in these monomethylases and dimethylases for histone arginine that is induced by *SETD4* KO may account for the biological function difference between *SEDT4* KO and WT BMSCs, as illustrated in Fig. 7.

Discussion

To explore the contribution and genomic methylation profiles of SEDT4 in BMSCs, we first established SETD4 KO mice using CRISPR/Cas9 technology, and these SETD4 KO mice showed a 4,044 bp deletion in exons 6–8 and significant inhibition of SETD4 at the translational level. Thus, these SETD4 KO mice provide a basis for further functional analysis. Morphologically, SETD4 KO BMSCs displayed no obvious difference with WT BMSCs, along with its immunophenotype. We focused on the proliferation, paracrine angiogenic factors and differentiation potentials, and our results provide the first evidence regarding the role of methyltransferase SETD4 in BMSCs biology.

High cell viability is a crucial determining factor in stem cell-based regeneration medicine. We found that SETD4 deficiency was beneficial for BMSCs proliferation, as evidenced by the CCK-8 assay results. Furthermore, we found that SETD4 KO up-regulated CDK6, cyclinA2 and cycinD1, and down-regulated P21 expression. Because these proteins were strongly associated with cell cycle progression, we can assume that SETD4 KO enhances BMSCs proliferation mainly through mediating cell cycle-associated proteins expression. We noticed that apoptosis-associated proteins such as Bcl2 and Caspase3 also changed, but no active Caspase3 was detected. It seems likely that inhibition of apoptosis may not be the key factor for SETD4 KO-induced BMSCs viability. An early report indicated that high expression of SETD4 promoted breast cancer cell proliferation without affecting the apoptosis[4]. Our current results suggest SETD4 deficiency leads to BMSCs proliferation without affecting the apoptosis. Very recently, Ye S and colleagues reported SETD4 overexpressed breast cancer stem cells deserved low Ki67 expression when compared with SETD4 low expressed breast cancer stem cells; they concluded SETD4 controls breast cancer stem cell quiescence [6]. Our current research found that SETD4 KO BMSCs retain high cell proliferative potentials, which is consistent with Ye S's report on cell proliferation characteristics. Interestingly, SETD4 KO also led to injured BMSCs migration. The morphology of cells in WT and SETD4 KO groups is very similar; thus, the reason for SETD4 KO-inhibited cell migration remains unsolved.

We next analyzed the effects of SETD4 KO on BMSC paracrine pro-angiogenic factors. Angiogenic factors like VEGF, TGF-β1, angiogenin-1 and bFGF contribute greatly to injured tissue recovery through mediating angiogenesis, and BMSCs process the ability of paracrine of angiogenic factors, which has been demonstrated by many investigations [18–21]. To our surprise, the current investigation showed that SETD4 KO dramatically attenuated BMSC producing VEGF at transcription and translation levels. Functionally, conditional medium enriched in supernatants from SETD4 KO BMSCs indeed led to a weakened tube formation capability of HUEVCs. This decrease in the ability of paracrine angiogenic factors suggests the functional damage of SETD4 KO cells in tissue injury transplantation. We plan to address this question in future in vivo experiment. A very recent investigation indicated SETD4 was positively involved in the release of cytokines like IL-6 and TNF-α in lipopolysaccharide-treated macrophages [8], highlighting the role of SETD4 in the immune and inflammatory response. Given that BMSCs were also involved in the macrophage-mediated inflammatory response [22], our current study provides novel molecular insights into epigenetic-modified immune response.

Directed differentiation is an important focus of BMSC function research. In this study, we investigated the myogenic differentiation potential of BMSCs and conducted experiments using mature myogenic differentiation induction protocols [23, 24]. Especially, for better efficiency, we combined 5-Aza with TGF-β1 to induce myogenic differentiation. The outcomes supported the notion that SETD4 was a requirement for myogenic differentiation in BMSCs, as elucidated by the abrogated expression of markers in cardiomyocytes (Nkx2.5, Gata-4, Mef2α, ANP, cTnT and CX43) and SMC (α-SMA, SM22α) in SETD4 KO cells. The exact reasons for the SETD4 KO-attenuated differentiation potentials were not clear. Change in genomic methylation status may alter the activity of differentiation linage-determined transcription factors [25–27], which may help in elucidating this phenotype. We take cardiomyocyte differentiation factors Nkx2.5 and Gata4 as a sample for discussion below.

Given that SETD4 is a methyltransferase, changes in the expression level of SETD4 may result in changes in the methylation status of the genome. We therefore assessed the status of genomic methylation in SETD4 KO and WT cells. Using the RRBS method, we obtained the overall trend in genomic methylation and differentially methylated CpG sites and DMR. Compared with WT BMSCs, SETD4 KO led to 0.47% decrease in the average methylation of all CpG sites, suggesting that the single deletion of SETD4 has a limited effect on the overall genomic methylation. In fact, in addition to SETD4, there are numerous other factors that serve in regulatory genomic methylation [28–30]. Even SETD4 KO just led to a very small change in the average methylation in genomic CpG sites; this change yet covers 96,331 differential CpG sites and 8692 DMRs, with part of them settling in genes' promoter region. Such a large number of differential methylated CpG sites and DMRs imply the complexity of gene expression and regulation.

To obtain potential functional and signaling pathways for differentially methylated CpG sites and DMRs in BMSCs after SETD4 KO, we performed GO and KEGG enrichment and annotation analysis. GO analysis indicated total 270 GO terms were enriched, which included 181 biological process, 35 cellular component and 44 molecular function terms. Regarding biological process classification, the top three GO terms were GO:0007275 ~ multicellular organism development; GO:0006355 ~ regulation of transcription, DNA-templated; and GO:0006351 ~ transcription, DNA-templated. A total of 560 enriched differential molecular located membrane (GO:0016020) in cellular component classification, indicating SETD4 KO affected downstream protein cellular location. GO:0005667 ~ transcription factor complex suggested SETD4 acts as a coupling in protein binding. GO:0043565 ~ sequence-specific DNA binding, GO:0005515 ~ protein binding and GO:0003677 ~ DNA binding were the top three GO terms in molecular function classification. Interestingly, we noticed enhanced GO:0007165 ~ signal transduction, GO:0030154 ~ cell differentiation, GO:0016477 ~ cell migration, GO:0001525 ~ angiogenesis and GO:0008283 ~ cell proliferation that were closely related to BMSC biology. These enriched differential GO terms provide a cue for elucidating SETD4 biological function. Regarding KEGG signaling, there were enriched 62 KEGG signaling pathways including conical mmu04151 ~ PI3K/Akt signaling pathways, mmu04310 ~ Wnt signaling pathways, mmu04350 ~ TGF-β signaling pathways, mmu04010 ~ MAPK signaling pathways and mmu04024 ~ cAMP signaling pathways. A total of 34 pathways were statistically significant. Among them, mmu04024 ~ cAMP signaling pathway was ranked as the top one. Interestingly, the relationship between cAMP signaling pathway and BMSCs has been documented [31]. In addition, Rap1 signaling pathway[32], regulation of actin cytoskeleton[33], signaling pathways regulating pluripotency of stem cells[34], focal adhesion[35], Hippo signaling pathway [36] and MAPK signaling pathway[37] that enriched in the current investigation have been reported to be closely related to stem cell biology. The results of GO and KEGG bioinformatics analysis suggest that the differentially methylated CpG islands and DMRs caused by SETD4 KO contain complex mechanisms that regulate BMSC biology.

We validated the expression of some interesting genes that are linked to differential methylation in promoter regions. We selected Nkx2.5, Gata4, Gli2, Grem2, E2f7, Map7, Nr2f2, Shox2, Foxo6, Klf14 and Dyrk3 as objectives. Among them, Nkx2.5 and Gata4 were tightly associated with cardiogenic differentiation [38]. Gli2[39], Grem2[40], E2f7[41], Nr2f2[42] and Shox2[43] are also related to stem cell

biology. Interestingly, SETD4 KO significantly changed the transcript of these genes. Among these genes, Gli2, E2f7, Shox2 and Klf14 were up-regulated, and the remaining genes were down-regulated. We found that all these genes contain multiple differentially methylated CpG sites in its promoter region. A dogmatic notion suggests that hypermethylation conventionally leads to gene silence, while hypomethylation generally results in gene activation. Since these genes contain multiple differentially methylated CpG sites, we did not test which CpG site plays the key role in SETD4 KO-induced changes in gene expression. In fact, total 96,331 differentially methylated CpG sites and 8692 DMRs were obtained in our study; these large numbers of differentially methylated CpG sites and DMRs undoubtedly cause a complex signal network and finally interfere with the biological function of BMSCs.

Finally, considering that SETD4 serves as a methyltransferase for histones, we thus tested the change of site-specific methylation of histone 3 (H3) and histone (H4). The results indicate that SETD4 KO obviously changed the levels of some HKMTs including H4K20me1, H4K20me2, H3K4me1, H3K4me2, H3K36me1, H3K36me2, H3K79me1 and H3K79me2, whereas no significant change was observed in the histone arginine trimethyltransferase. Thus, we hypothesized that the role of SETD4 in the biological function of BMSCs is mainly related to the change of genomic methylation level caused by the change of these monomethylases and dimethylases. The diagram of mechanism is illustrated in Fig. 7.

Conclusions

In summary, this is the first investigation to explore the biological functions of *SETD4* in BMSCs and its impact on genomic methylation. Our results demonstrate that *SETD4* plays a crucial role in proliferation, migration, paracrine and myogenic differentiation of BMSCs. Even though *SETD4* changes minimal level in overall genomic methylation, it still leads to large differential methylated CpG sites and DMRs, which results in numerous changes in cellular functions and signaling pathways. This investigation provides an experimental basis for BMSC-based regeneration medicine through epigenetic modification.

Declarations

Ethics approval and consent to participate

All animal procedures were conducted in accordance with protocols approved by the Institutional Animal Care and Use Committee (IACUC) of Guangdong Medical University.

Consent for publication

Not applicable.

Availability of data and materials

All data generated or analyzed during this study are included in this published article and its supplementary information files.

Competing interests

The authors declare that they have no competing interests.

Funding

This work was financially supported by the National Natural Science Foundations of China (No. 81670254, 81770487 and 91939107), and YangFan Plan of Guangdong Province (4YF16007G). The funding bodies have no role in the design of the study and collection, analysis, and interpretation of data and in writing the manuscript.

Authors' contributions

Conception and design: WJ, JLG, SJZ; Collection and/or assembly of data: XML, CXW, ZMS, SYZ, YZ, JLY, MYF, YPH, JCX and AXZ; Data analysis and interpretation: XML, ZHS; Financial support: WJ, JLG; Provision of study material: YPH and RJL; Manuscript writing: WJ, SJZ; Final approval of manuscript: all of the authors.

Acknowledgements

The authors thank GeneChem Corporation (Shanghai) for the help provided in DNA methylation analysis. The author would like to thank Accdon-LetPub for editing the English for the manuscript.

Author details

[1]Department of Pathology, School of Basic Medicine Sciences, Guangdong Medical University, Zhanjiang 524023, China; [2]Hainan Provincial Key Laboratory for Tropical Cardiovascular Diseases Research & Key Laboratory of Emergency and Trauma of Ministry of Education, Institute of Cardiovascular Research of the First Affiliated Hospital, Hainan Medical University, Haikou 571199.

Abbreviations

5-Aza: 5-Aza-2’-deoxycytidine; BMSCs: Bone marrow mesenchymal stem cells; DMRs: Differential methylation regions; HKMTs: Histone lysine methyltransferases; HRMTs: Arginine methyltransferases; KO: Knock out; RRBS: Reduced Representation Bisulfite Sequencing; STED4: SET domain-containing protein 4; TGF-b1: Transforming growth factor b1; WT: Wild type.

References

1. Hyun K, Jeon J, Park K, Kim J. Writing, erasing and reading histone lysine methylations. Exp Mol Med. 2017; 49:e324.
2. Rose NR, Klose RJ. Understanding the relationship between DNA methylation and histone lysine methylation. Biochimica et biophysica acta. 2014;1839:1362-72.

3. Wesche J, Kuhn S, Kessler BM, Salton M, Wolf A. Protein arginine methylation: a prominent modification and its demethylation. Cell Mol Life Sci. 2017;74:3305-15.
4. Faria JA, Corrêa NC, de Andrade C, de Angelis Campos AC, Dos Santos Samuel de Almeida R, Rodrigues TS, de Goes AM, Gomes DA, Silva FP. SET domain-containing Protein 4 (SETD4) is a Newly Identified Cytosolic and Nuclear Lysine Methyltransferase involved in Breast Cancer Cell Proliferation. J Cancer Sci Ther. 2013;5:58-65.
5. Zhu S, Xu Y, Song M, Chen G, Wang H, Zhao Y, Wang Z, Li F. PRDM16 is associated with evasion of apoptosis by prostatic cancer cells according to RNA interference screening. Mol Med Rep. 2016;14:3357-61.
6. Ye S, Ding YF, Jia WH, Liu XL, Feng JY, Zhu Q, Cai SL, Yang YS, Lu QY, Huang XT, Yang JS, Jia SN, Ding GP, Wang YH, Zhou JJ, Chen YD, Yang WJ. SET domain-containing protein 4 epigenetically controls breast cancer stem cell quiescence. Cancer Res. 2019;79:4729-43.
7. Dai L, Ye S, Li HW, Chen DF, Wang HL, Jia SN, Lin C, Yang JS, Yang F, Nagasawa H, YangWJ. SETD4 Regulates Cell Quiescence and Catalyzes the Trimethylation of H4K20 during Diapause Formation in Artemia. Mol Cell Biol. 2017;37:e00453-16.
8. Zhong Y, Ye P, Mei Z, Huang S, Huang M, Li Y, Niu S, Zhao S, Cai J, Wang J, Zou H, Jiang Y, Liu J. The novel methyltransferase SETD4 regulates TLR agonist-induced expression of cytokines through methylation of lysine 4 at histone 3 in macrophages. Mol Immunol. 2019;114:179-88.
9. Liang X, Ding Y, Zhang Y, Tse HF, Lian Q. Paracrine mechanisms of mesenchymal stem cell-based therapy: current status and perspectives. Cell Transplant. 2014;23:1045-59.
10. Mortada I, Mortada R. Epigenetic changes in mesenchymal stem cells differentiation. Eur J Med Genet. 2018; 61:114-8.
11. Teven CM, Liu X, Hu N, Tang N, Kim SH, Huang E, Yang K, Li M, Gao JL, Liu H, Natale RB, Luther G, Luo Q, Wang L, Rames R, Bi Y, Luo J, Luu HH, Haydon RC, Reid RR, He TC. Epigenetic regulation of mesenchymal stem cells: a focus on osteogenic and adipogenic differentiation. Stem Cells Int. 2011; 2011:201371.
12. Shi S, Wu X, Wang X, Hao W, Miao H, Zhen L, Nie S. Differentiation of Bone Marrow Mesenchymal Stem Cells to Cardiomyocyte-Like Cells Is Regulated by the Combined Low Dose Treatment of Transforming Growth Factor-beta1 and 5-Azacytidine. Stem Cells Int. 2016; 2016:3816256.
13. Ozkul Y, Galderisi U. The Impact of Epigenetics on Mesenchymal Stem Cell Biology. J Cell Physiol. 2016;231:2393-401.
14. Ding R, Jiang X, Ha Y, Wang Z, Guo J, Jiang H, Zheng S, Shen Z, Jie W. Activation of Notch1 signalling promotes multi-lineage differentiation of c-Kit(POS)/NKX2.5(POS) bone marrow stem cells: implication in stem cell translational medicine. Stem Cell Res Ther. 2015; 6:91.
15. Soleimani M, Nadri S. A protocol for isolation and culture of mesenchymal stem cells from mouse bone marrow. Nat Protoc. 2009; 4:102-6.
16. Shen Z, Liao X, Shao Z, Feng M, Yuan J, Wang S, Gan S, Ha Y, He Z, Jie W. Short-term stimulation with histone deacetylase inhibitor trichostatin a induces epithelial-mesenchymal transition in

nasopharyngeal carcinoma cells without increasing cell invasion ability. BMC cancer. 2019;19:262.

17. Wu Y, Shen Z, Wang K, Ha Y, Lei H, Jia Y, Ding R, Wu D, Gan S, Li R, Luo B, Jiang H, Jie W. High FMNL3 expression promotes nasopharyngeal carcinoma cell metastasis: role in TGF-beta1-induced epithelia-to-mesenchymal transition. Sci Rep. 2017;7:42507.
18. Guo S, Zhen Y, Wang A. Transplantation of bone mesenchymal stem cells promotes angiogenesis and improves neurological function after traumatic brain injury in mouse. Neuropsychiatr Dis Treat. 2017;13:2757-65.
19. Blondiaux E, Pidial L, Autret G, Rahmi G, Balvay D, Audureau E, Wilhelm C, Guerin CL, Bruneval P, Silvestre JS, Menasché P, Clément O. Bone marrow-derived mesenchymal stem cell-loaded fibrin patches act as a reservoir of paracrine factors in chronic myocardial infarction. J Tissue Eng Regen Med. 2017;11:3417-27.
20. Carrion B, Kong YP, Kaigler D, Putnam AJ. Bone marrow-derived mesenchymal stem cells enhance angiogenesis via their alpha6beta1 integrin receptor. Exp Cell Res. 2013; 319:2964-76.
21. Kaigler D, Krebsbach PH, Polverini PJ, Mooney DJ. Role of vascular endothelial growth factor in bone marrow stromal cell modulation of endothelial cells. Tissue Eng. 2003; 9:95-103.
22. Ma QL, Fang L, Jiang N, Zhang L, Wang Y, Zhang YM, Chen LH. Bone mesenchymal stem cell secretion of sRANKL/OPG/M-CSF in response to macrophage-mediated inflammatory response influences osteogenesis on nanostructured Ti surfaces. Biomaterials. 2018; 154:234-47.
23. Sun P, Jia K, Zheng C, Zhu X, Li J, He L, Siwko S, Xue F, Liu M, Luo J, Loss of Lgr4 inhibits differentiation, migration and apoptosis, and promotes proliferation in bone mesenchymal stem cells. J Cell Physiol. 2019;234:10855-67.
24. Guo X, Bai Y, Zhang L, Zhang B, Zagidullin N, Carvalho K, Du Z, Cai B. Cardiomyocyte differentiation of mesenchymal stem cells from bone marrow: new regulators and its implications. Stem Cell Res Ther, 2018; 9:44.
25. Cakouros D, Hemming S, Gronthos K, Liu R, Zannettino A, Shi S, Gronthos S. Specific functions of TET1 and TET2 in regulating mesenchymal cell lineage determination. Epigenetics Chromatin. 2019; 12:3.
26. Takada I, Kouzmenko AP, Kato S. Molecular switching of osteoblastogenesis versus adipogenesis: implications for targeted therapies. Expert Opin Ther Targets. 2009, 13:593-603.
27. Zhang Y, Ma C, Liu X, Wu Z, Yan P, Ma N, Fan Q, Zhao Q. Epigenetic landscape in PPARgamma2 in the enhancement of adipogenesis of mouse osteoporotic bone marrow stromal cell. Biochim Biophys Acta. 2015; 1852:2504-16.
28. Edwards JR, Yarychkivska O, Boulard M, Bestor TH. DNA methylation and DNA methyltransferases. Epigenetics Chromatin. 2017;10:23.
29. Kimura H. Histone modifications for human epigenome analysis. J Hum Genet. 2013; 58:439-45.
30. Du J, Johnson LM, Jacobsen SE, Patel DJ. DNA methylation pathways and their crosstalk with histone methylation. Nat Rev Mol Cell Biol. 2015;16:519-32.

31. Chen B, Lin T, Yang X, Li Y, Xie D, Cui H. Intermittent parathyroid hormone (1-34) application regulates cAMP-response element binding protein activity to promote the proliferation and osteogenic differentiation of bone mesenchymal stromal cells, via the cAMP/PKA signaling pathway. Exp Ther Med. 2016;11:2399-406.
32. Ding Y, Liang X, Zhang Y, Yi L, Shum HC, Chen Q, Chan BP, Fan H, Liu Z, Tergaonkar V, Qi Z, Tse HF, Lian Q. Rap1 deficiency-provoked paracrine dysfunction impairs immunosuppressive potency of mesenchymal stem cells in allograft rejection of heart transplantation. Cell Death Dis. 2018;9:386.
33. Sen B, Uzer G, Samsonraj RM, Xie Z, McGrath C, Styner M, Dudakovic A, van Wijnen AJ, Rubin J. Intranuclear Actin Structure Modulates Mesenchymal Stem Cell Differentiation. Stem Cells. 2017;35:1624-35.
34. Okita K, Yamanaka S. Intracellular signaling pathways regulating pluripotency of embryonic stem cells. Curr Stem Cell Res Ther. 2006;1:103-11.
35. Hu Y, Lu J, Xu X, Lyu J, Zhang H. Regulation of focal adhesion turnover in SDF-1alpha-stimulated migration of mesenchymal stem cells in neural differentiation. Sci Rep. 2017;7:10013.
36. Mo JS, Park HW, Guan KL. The Hippo signaling pathway in stem cell biology and cancer. EMBO Rep. 2014;15:642-56.
37. Jiao F, Tang W, Huang H, Zhang Z, Liu D, Zhang H, Ren H. Icariin Promotes the Migration of BMSCs In Vitro and In Vivo via the MAPK Signaling Pathway. Stem Cells Int. 2018;2018:2562105.
38. Sanchez-Freire V, Lee AS, Hu S, Abilez OJ, Liang P, Lan F, Huber BC, Ong SG, Hong WX, Huang M, Wu JC. Effect of human donor cell source on differentiation and function of cardiac induced pluripotent stem cells. J Am Coll Cardiol. 2014;64:436-48.
39. Zhao C, Cai S, Shin K, Lim A, Kalisky T, Lu WJ, Clarke MF, Beachy PA. Stromal Gli2 activity coordinates a niche signaling program for mammary epithelial stem cells. Science. 2017; 356: eaal3485.
40. Bylund JB, Trinh LT, Awgulewitsch CP, Paik DT, Jetter C, Jha R, Zhang J, Nolan K, Xu C, Thompson TB, Kamp TJ, Hatzopoulos AK. Coordinated Proliferation and Differentiation of Human-Induced Pluripotent Stem Cell-Derived Cardiac Progenitor Cells Depend on Bone Morphogenetic Protein Signaling Regulation by GREMLIN 2. Stem Cells Dev. 2017; 26:678-93.
41. Dehghanian F, Hojati Z, Esmaeili F, Masoudi-Nejad A. Network-based expression analyses and experimental validations revealed high co-expression between Yap1 and stem cell markers compared to differentiated cells. Genomics. 2019;111:831-9.
42. Rosa A, Brivanlou AH. A regulatory circuitry comprised of miR-302 and the transcription factors OCT4 and NR2F2 regulates human embryonic stem cell differentiation. EMBO J. 2011;30:237-48.
43. Ionta V, Liang W, Kim EH, Rafie R, Giacomello A, Marban E, Cho HC. SHOX2 overexpression favors differentiation of embryonic stem cells into cardiac pacemaker cells, improving biological pacing ability. Stem Cell Rep. 2015;4:129-42.

Additional Files

Additional file 1: Figure S1. Quality control of RRBS assay. (A) Clean Reads distribution of mass per site; (B) the distribution of average quality values for clean reads; (C) maps of base A, T, C, G site in clean reads; (D) Distribution of actual GC content and theoretical GC content per read; (E) Percentage of each site in reads; (F) Sequencing length map.

Additional file 2: Table S1. Basic statistical results of samples methylation sequencing.

Additional file 3: Figure S2. Representative histogram of CpG Coverage and % CpG methylation. (A) Histogram of CpG Coverage; (B) Histogram of % CpG methylation. WT: K419, K420 and K421; SETD4 KO: K422, K423 and K424.

Additional file 4: Table S2. Full list for methylated CpG sites.

Additional file 5: Table S3. Full list for DMRs.

Additional file 6: Table S4. Complete list for enriched GO terms.

Additional file 7: Table S5. Complete list for enriched KEGG signaling.

Additional file 8: Table S6. Differentially methylated CpG sites invalidated genes' promoter regions.

Figures

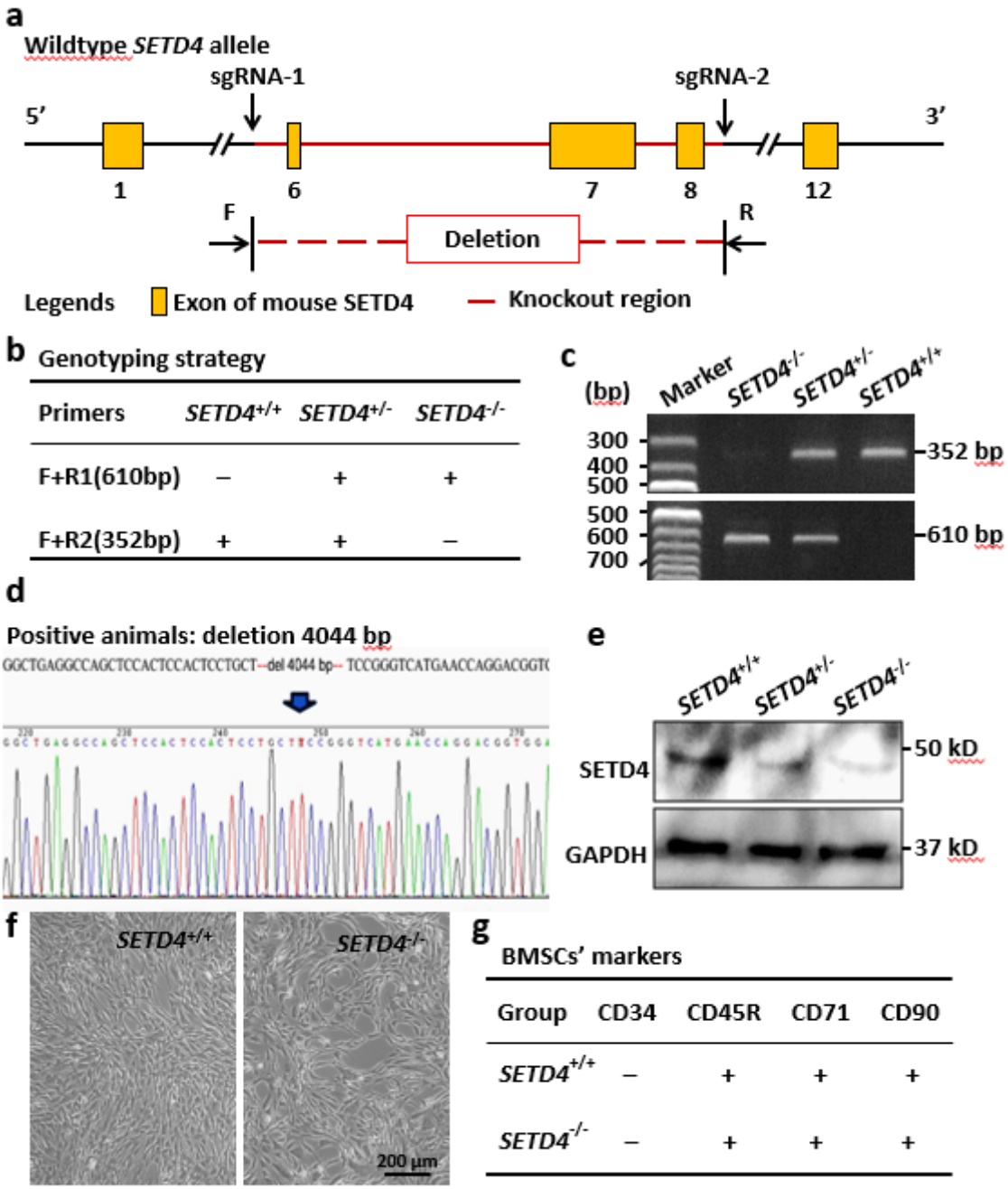

Figure 1

Isolation and identification of BMSCs from WT and SETD4-KO mice. a Schematic diagram of editing mouse SETD4 allele through CRISPR/Cas9 technology. b Genotyping strategy for mouse identification. c Agarose electropherogram of PCR products of representative various genotype mice. d Sequencing results of a positive mouse. e Western blot results of SETD4 protein in various genotypic mice. f Morphology of BMSCs. Bar = 50 μm. g Immunophenotype of BMSCs detected by flow cytometry.

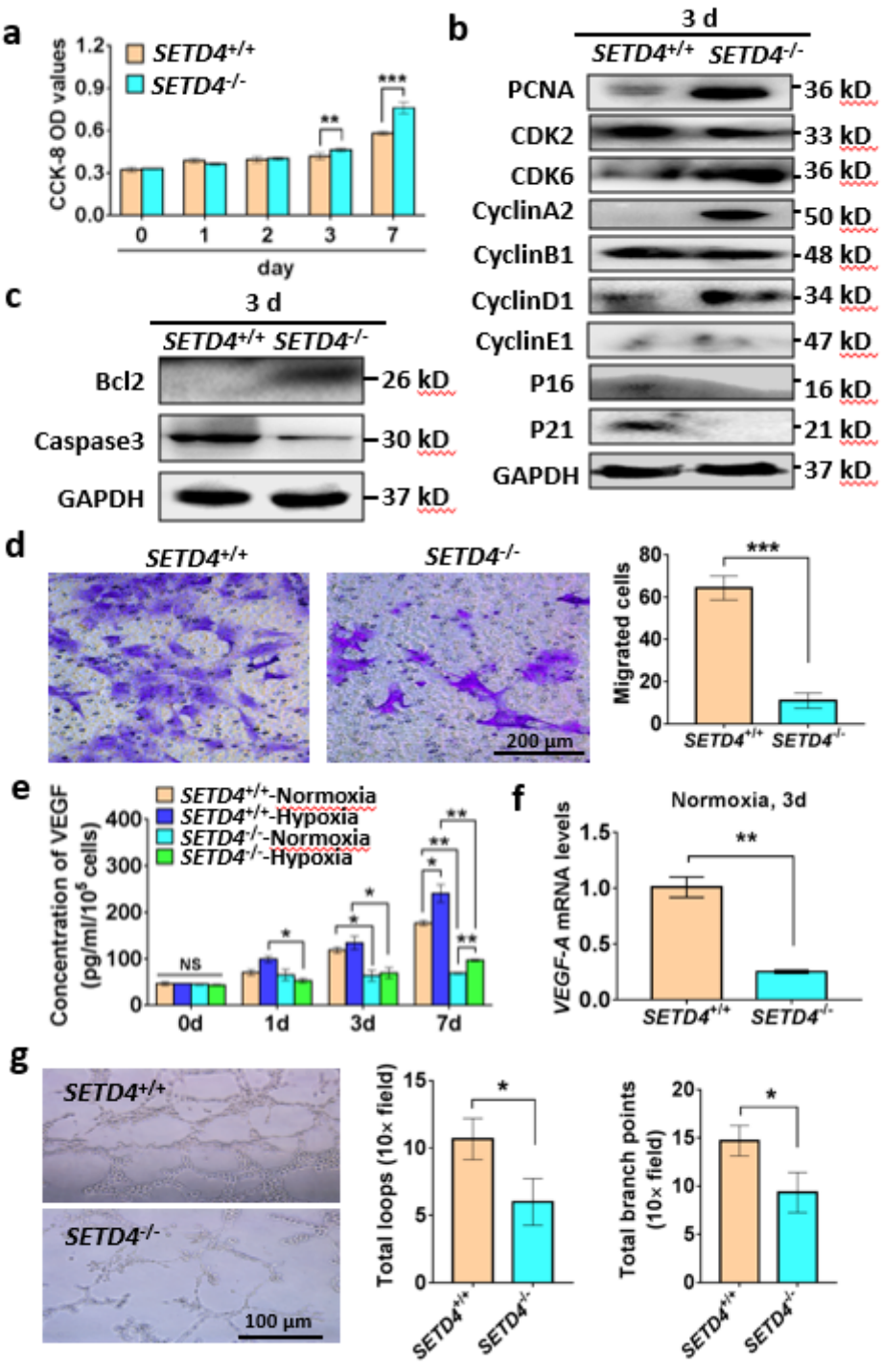

Figure 2

Effects of SETD4 on proliferation, migration and proangiogenic of BMSCs. a CCK-8 assay was used to test BMSCs' viability. n = 3, **P<0.01, ***P<0.001. b Representative western blot results of cell cycle-associated proteins. c Representative western blot results of apoptosis-associated proteins. d Results of transwell chamber migration assay. n = 3, ***P<0.001. e ELISA outcomes of BMSC secretion of VEGF in supernatants. n = 3, *P<0.05, **P<0.01, ***P<0.001. f Real-time PCR results of VEGF-A mRNA levels in

BMSCs. n = 3, **P<0.01. g Tube formation of HUEVCs treated with BMSC conditional medium. n = 3, *P<0.05.

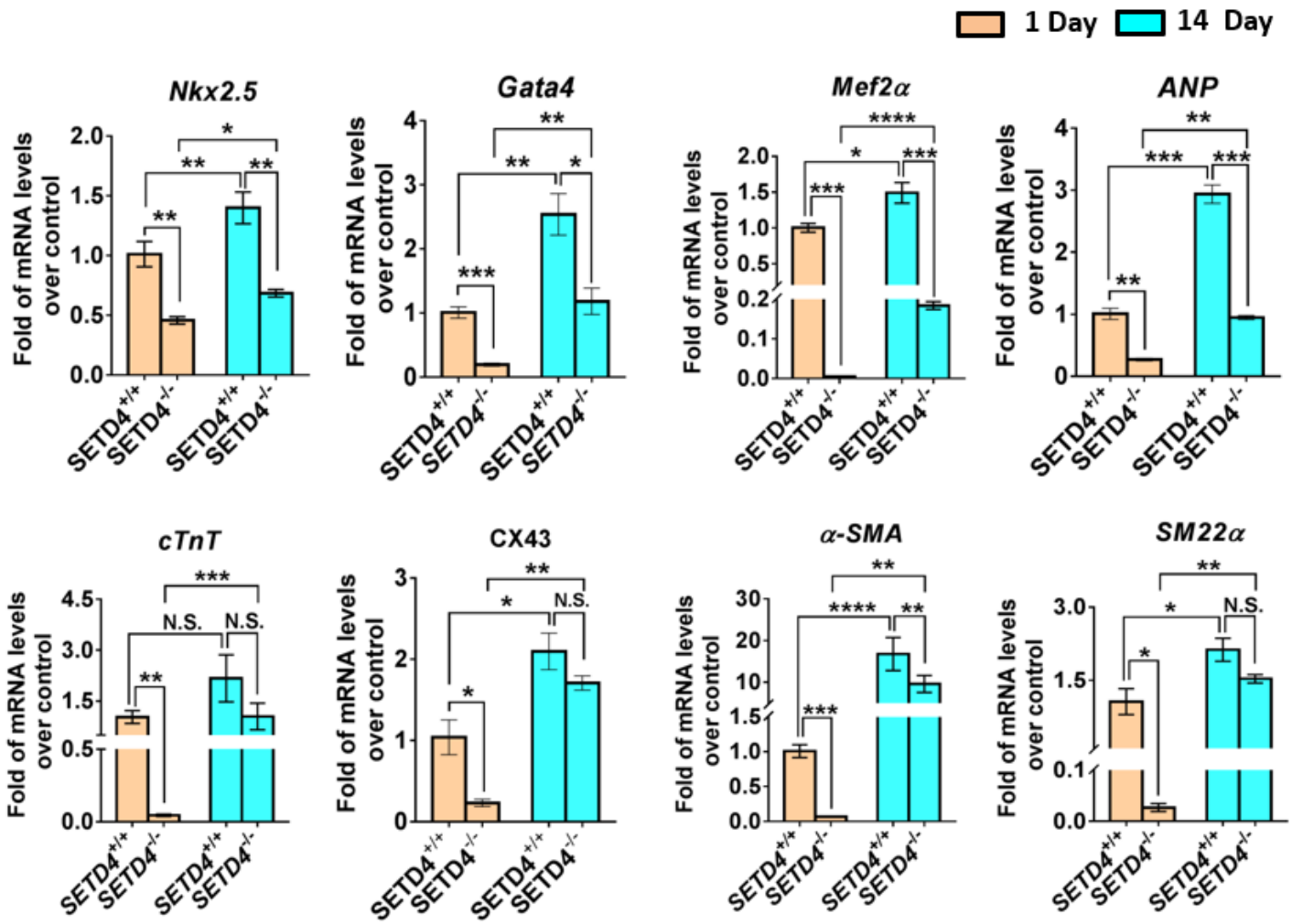

Figure 3

Myogenic differentiation of BMSCs. BMSCs were treated with 5'-Aza plus TGF-β1 for 14 d as elucidated in the methods section, and cardiomyocyte markers (Nkx2.5, Gata4, Mef2A, ANP, CX43) and smooth muscle cell lineage marker (α-SMA, SM22α) were evaluated by real-time PCR. n = 3, *P<0.05; **P<0.01; ***P<0.001; N.S., non-significant.

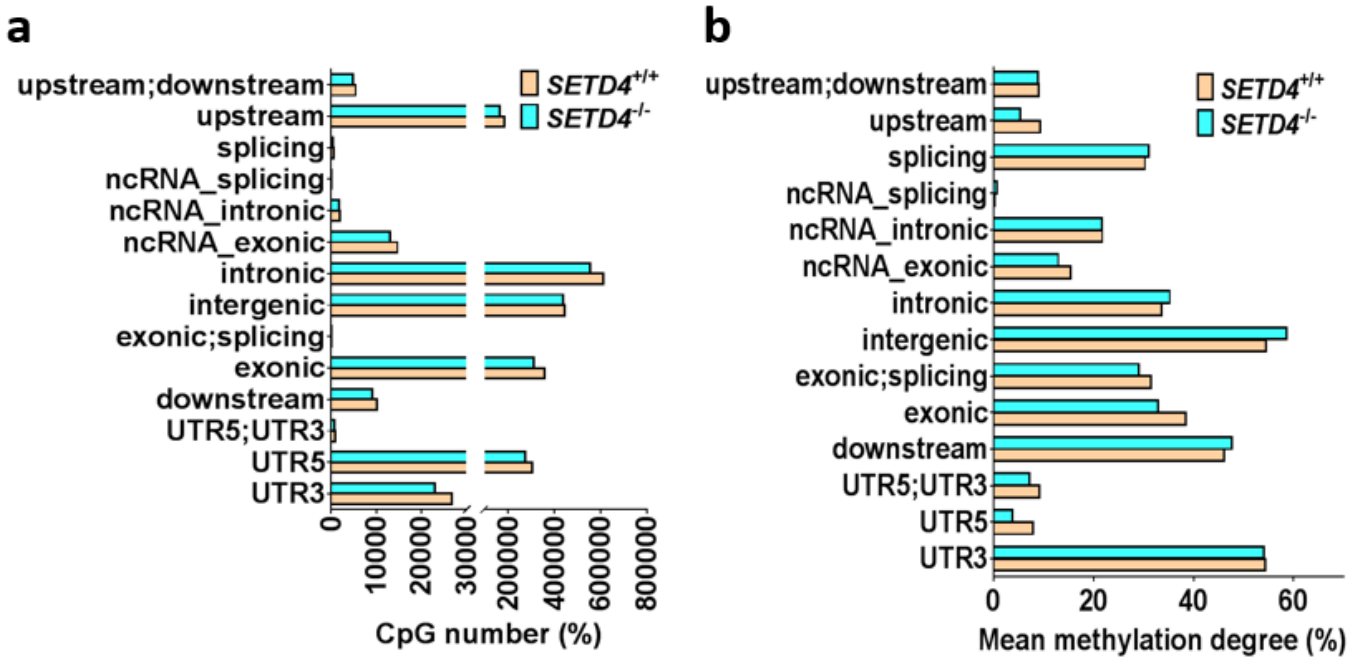

c Number of single CpG different methylation site

$SETD4^{-/-} - SETD4^{+/+} > 25\%$	$SETD4^{-/-} - SETD4^{+/+} < -25\%$	Total
32216	64115	96331

d Number of differential methylation regions (DMRs)

$SETD4^{-/-} - SETD4^{+/+} > 25\%$, $P \leq 0.01$	$SETD4^{-/-} - SETD4^{+/+} < -25\%$, $P \leq 0.01$	Total	Promoter region
5055	3637	8692	2247

Figure 4

Overall genomic methylation status of BMSCs. WT BMSCs and SETD4 KO BMSCs were subjected to analysis of genomic methylation by RRBS, and the number of identified CpG islands in elements of the genome (a) and mean methylation degree in genomic elements (b) are shown. c Statistical results of the number of single CpG different methylation site as per the standard KO-WT>25% or KO-WT<-25%. d Statistical results of the number of DMR as per the standard KO-WT>25% & P<0.01, or KO-WT<-25% & P<0.01.

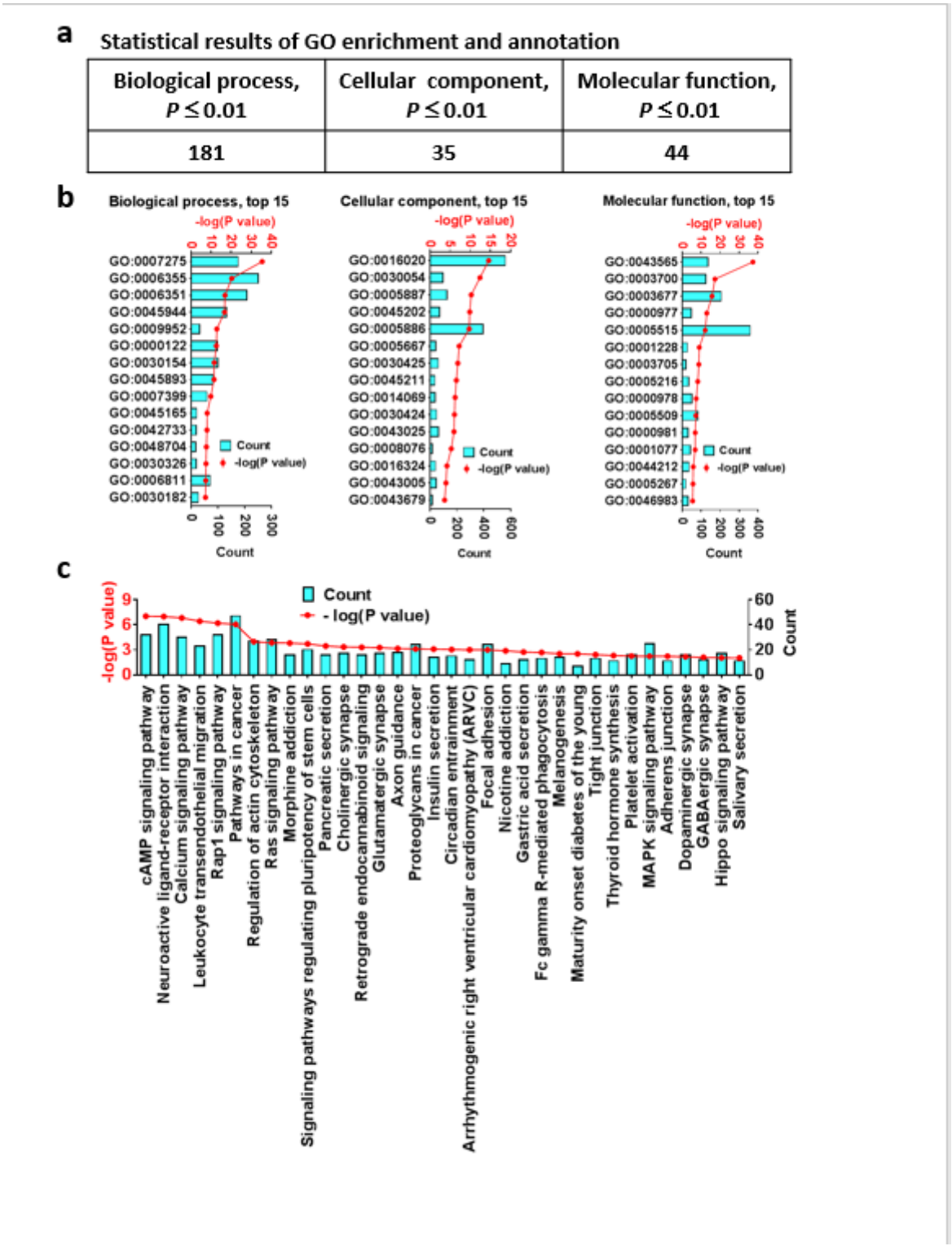

Figure 5

GO and KEGG analysis of differential methylated CpG sites and DMRs in BMSCs. a Statistical results of enriched significant GO terms. b Top 15 GO terms in biological process, cellular component and molecular function that enriched in differential methylated CpG sites and differential methylated regions in promoters. For the detail of each GO term, see Table S4 (Additional file 6). c Total 34 differential KEGG signals were enriched in differential methylated CpG sites and DMRs in promoters. These KEGG signals

were arranged in P values converted −log (P values). For the enriched genes' detail of each KEGG signal, see Table S5 (Additional file 7).

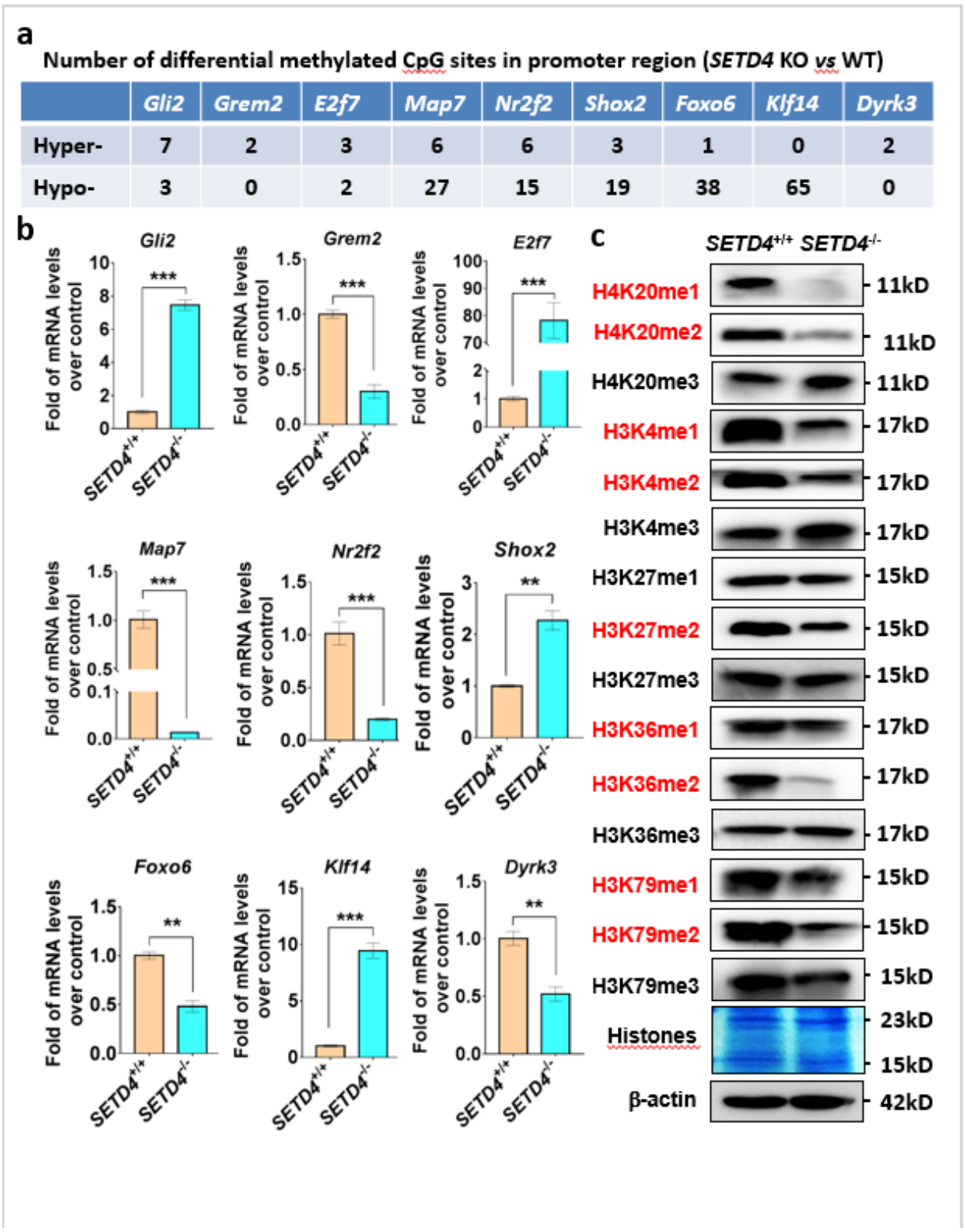

	Gli2	Grem2	E2f7	Map7	Nr2f2	Shox2	Foxo6	Klf14	Dyrk3
Hyper-	7	2	3	6	6	3	1	0	2
Hypo-	3	0	2	27	15	19	38	65	0

Figure 6

Validation of representative genes and HKMTs. a The number of differential methylated CpG sites in the promoter region of validated genes. A total of nine representative genes with differential methylated CpG sites in the promoter region were used to test its mRNA levels. The number of hypermethylated (KO-

WT=25% to 100%, P<0.01) or hypomethylated (KO-WT=-25% to -100%, P<0.01) CpG sites of each gene were included. b Real-time PCR results of validated nine genes mRNA levels. n = 3, **P<0.01; ***P<0.001. c Representative western blot results of sets of HKMTs. HKMTs in red color were significantly changed.

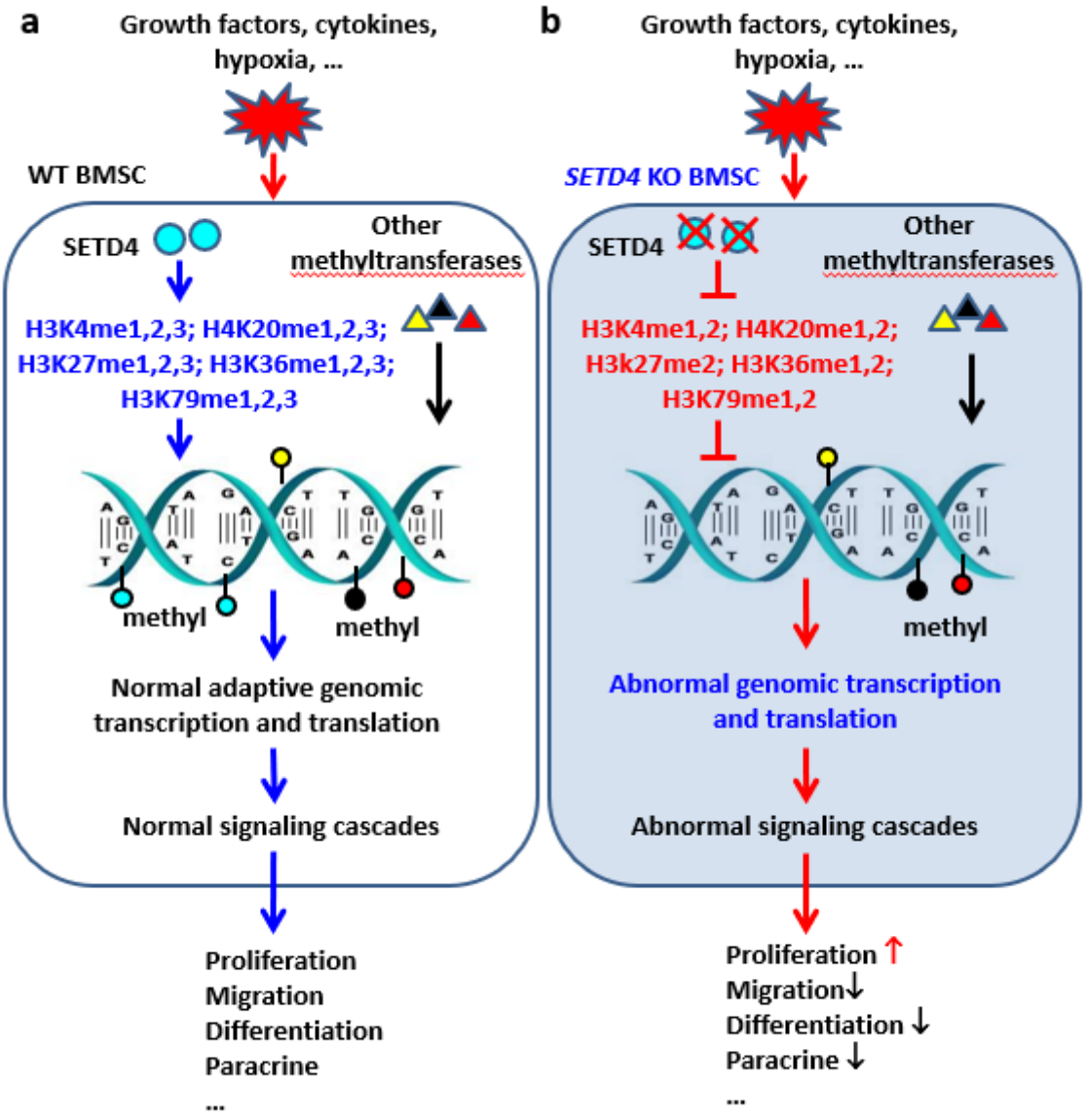

Figure 7

Schematic diagram of the role and mechanism of SETD4 in BMSC biology. a In WT BMSCs, SETD4 with other methylation catalytic enzymes changes the genomic methylation at specific CpG sites. Induced by growth factors, cytokines hypoxia and other stimulating factors, WT cells display a normal adaptive genomic transcription and translation process and then lead to activation of normal signaling cascades, which in turn produces adaptive cellular biological function such as proliferation, migration, differentiation and paracrine. b In SETD4 KO BMSCs, due to loss of SETD4, a set of HKMTs including

H4K20me1, H4K20me2, H3K4me1, H3K4me2, H3K27me2, H3K36me1, H3K36me2, H3K79me1 and H3K79me2 were inhibited. Induced by growth factors, cytokines, hypoxia and other stimulating factors, SETD4 KO cells display an abnormal genomic transcription and translation process and then lead to activation of abnormal signaling cascades, which in turn increases proliferation and decreases migration, differentiation and paracrine effects.

Supplementary Files

This is a list of supplementary files associated with this preprint. Click to download.

- Additionalfile7TableS5.xlsx
- Additionalfile4TableS2.xlsx
- Additionalfile5TableS3.xlsx
- Additionalfile6TableS4.xlsx
- Additionalfile3FigureS2.pdf
- Additionalfile8TableS6.xlsx
- Additionalfile2TableS1.xlsx
- Additionalfile1FigureS1.pdf